

8.92 MeV doublet and 8.98 MeV level in ^{15}O

D. Drain, B. Chambon, M. Lambert, C. Pastor, N. Persehaye, and J. L. Vidal

*Institut de Physique Nucléaire, Université Claude Bernard, Lyon-I, France**and IN2P3, 43 Bd du 11 novembre, 69621 Villeurbanne, France*

P. Midy

Laboratoire de Physique Théorique et Hautes Energies, Université Paris XI, 91405 Orsay, France

(Received 16 June 1976)

The analysis of excitation curves and angular correlations of the γ rays from the $^{14}\text{N}(p,\gamma)^{15}\text{O}$ reaction confirms the existence of a doublet at 8.92 MeV in ^{15}O . $J^\pi = 5/2^+$ and $J^\pi = 1/2^-$ assignments are determined for the spins and parities of the two members of this doublet. The 8.98 MeV level is found to have $J^\pi = 3/2^-$. This study was performed using a differentially pumped gas target of natural nitrogen. A comparison with ^{15}N levels and with theoretical results is discussed.

NUCLEAR REACTIONS $^{14}\text{N}(p, \gamma)$, $E = 1.742, 1806$ MeV. Measured $\sigma(E)$, $\gamma\gamma(\theta)$.
 ^{15}O levels deduced J , π . Natural gas target.

I. INTRODUCTION

Many studies of the excited states in ^{15}N and ^{15}O have been performed¹ and the correspondence between the analog states is now well established up to $E_x \simeq 8.7$ MeV in ^{15}O . Beyond this energy the situation is not so clear; in particular it is not clear for the ^{15}O levels at 8.92–8.98 MeV which are investigated here.

A study of the $^{14}\text{N}(p, p)$ reaction by Lambert *et al.*² has shown that the state at 8.92 MeV in ^{15}O is a doublet with $J^\pi = \frac{5}{2}^+$ for one member and $J^\pi = (\frac{1}{2}, \frac{3}{2})^-$ for the other. These determinations are consistent with other results obtained from the $^{13}\text{C}(^3\text{He}, n)^{15}\text{O}$ reaction studies,^{3–5} although the conclusions differ according to authors; Etten and Lenz³ give $J^\pi = (\frac{1}{2}, \frac{3}{2})^+$ for the 8.92 MeV level considered as a single level, but they do not rule out the presence of a $\frac{5}{2}^+$ state in the 9 MeV region. The analysis of Hinderlitter and Lochstet⁴ is consistent with the possible presence of a $\frac{1}{2}^-$ state at $E_x = 9$ MeV, while Honsaker *et al.*⁵ assign $J^\pi = \frac{1}{2}^-$ to the state at 8.92 MeV. Krone and Fiarman⁶ have examined the resonance structure in ^{15}O between 8.8 and 9.0 MeV and studied the excitation function of the γ rays following proton capture by ^{14}N ; they confirm the existence of a doublet with components corresponding to 8.920 and 8.925 MeV excitations. However, such a large difference between the energies is inconsistent with the $^{14}\text{N}(p, p)$ analysis of Ref. 2.

For the 8.98 MeV level, both $J^\pi = \frac{1}{2}^-$ and $J^\pi = \frac{3}{2}^-$ assignments have been proposed (Refs. 3 and 4, respectively, and Ref. 1).

By means of the $^{14}\text{N}(d, p)^{15}\text{N}$ reaction, Amokrane

*et al.*⁷ measured the spectroscopic factors for levels at 9.152, 9.155, and 9.22 MeV in ^{15}N and propose $J^\pi = \frac{3}{2}^-$, $\frac{5}{2}^+$, and $\frac{1}{2}^-$ for these three levels, respectively. Furthermore, they compare their neutron reduced widths with the proton reduced widths determined from the $^{14}\text{N}(p, p)$ study^{1,2} and conclude that these states may be the analog states of the 8.92 MeV doublet and 8.98 MeV level in ^{15}O (such a correspondence has also been suggested in Ref. 6, but is not supported by any spin measurement). This conclusion is in agreement with the shell-model calculations by Lie and Engeland⁸ who predicted three levels with $J^\pi = \frac{1}{2}^-$, $\frac{3}{2}^-$, and $\frac{5}{2}^+$ in that energy range, for the $A = 15$ mirror pair.

The purpose of this paper is to complete our previous (p, p) results² in order to definitively remove the spin ambiguities in ^{15}O , between $\frac{5}{2}^+$, $\frac{1}{2}^-$ and $\frac{5}{2}^+$, $\frac{3}{2}^-$ sets of spin for the doublet at 8.92 MeV and between $\frac{1}{2}^-$ and $\frac{3}{2}^-$ for the spin of the 8.98 MeV level, and to justify the correspondence with the analog states in ^{15}N . Thus, employing a gas target of natural nitrogen, we studied the $^{14}\text{N}(p, \gamma)$ reaction, reexamining the excitation functions and measuring angular correlations for the γ rays.

II. EXPERIMENTAL PROCEDURE

Many previous experiments^{3–6} were performed with solid nitrogen targets, prepared either by heating a tantalum backing in an atmosphere of ammonia, by evaporating a nitrogen compound onto a backing, or by sputtering tantalum onto a platinum backing in a discharge or nitrogen gas.

Such solid targets have many disadvantages:

(i) They are often too thick to study thin resonances, thus degrading energy resolution; (ii) they do not withstand the large beam currents required for correlation measurements; and (iii) the buildup of a carbon deposit introduces a change in the effective incident energy and degrades the energy resolution. To escape these difficulties, a gaseous target may be used; in a $^{14}\text{N}(p, \gamma)$ experiment Kuan *et al.*⁹ used a transmission cell containing nitrogen, the beam entrance and exit windows being made of molybdenum foils. Nevertheless, the entrance window introduced an uncertainty in the energy of the incident proton beam and such a transmission cell did not alleviate the problem of the carbon deposit.

The target used here is a differentially pumped gas target; this allows easy modifications in the target thickness and avoids contamination. The gas cell is a 2 cm high tantalum cylinder, with a 1 cm inside diameter and wall thickness of 2 mm. The incident proton beam enters this cell through an isolated diaphragm and is stopped in the wall of the cell (this permits a broad angular range, including 0° , for γ -ray detection). The pressure in the cell is typically 10–60 Torr. The first stage is pumped by a Roots blower with a pumping speed of 36 l/s at 10^{-1} Torr; the pressure is 10^{-1} – 6×10^{-1} Torr. The pressure in the second state, pumped by a mercury diffusion pump, is about 10^{-4} Torr. Between this second stage and the beam tube of the accelerator, a set of five diaphragms collimates the proton beam; lead blocks protect the detector from direct view of the impact points on the collimators. The isotropy of this chamber was tested with the well-known angular distribution of γ rays from the $^{15}\text{N}(p, \alpha\gamma)^{12}\text{C}$ reaction at $E_p = 1210$ keV (Ref. 10).

For the angular correlation measurements, a 92 cm³ Ge(Li) detector can rotate in the horizontal plane from 0° to 130° on one side of the beam axis and three 12.7 \times 15.2 cm NaI detectors, separated by 45° from each other in the horizontal plane can be rotated to cover the same angular range, but on the other side of the beam axis. The target-to-detector distances [10 cm for the Ge(Li) and 20 cm for the NaI] are large enough to avoid corrections due to the use of a nonpunctual target. This arrangement allows a study of the *A* and *B* geometries as defined by Fergusson.¹¹ The analogic pulses from the four detectors are sent into a multiplexer; timing signals from the Ge(Li) detector and from a (*i*th) NaI detector are sent in the *i*th time-to-pulse converter (TPC). The analogic outputs of the three TPC's are sent into the multiplexer. An OR circuit, placed at the logic outputs of the TPC interrogates the multiplexer when two

events are detected within the time range of one of the TPC's. The multiplexer then authorizes the sequential conversions of the analogic pulses by an analog-to-digital converter connected to a Hewlett-Packard 2116C computer. The events are recorded on magnetic tapes. The γ rays are detected by the three NaI detectors, each of them being in coincidence (defined by the TPC ranges) with the Ge(Li) detector placed at 90° . No energy window in the Ge(Li) spectra is fixed, thus the recorded events correspond to all possible cascades. Because of the use of three NaI detectors, only four measurements are necessary to obtain 12 points for each angular correlation. The angular correlation for one cascade is obtained by reading the events recorded on the magnetic tape, setting the necessary energy [Ge(Li)] and time (TPC) conditions. We subtracted the accidental coincidence spectra obtained by moving the window, in the TPC spectra, out of the true coincidence peak region. The geometries employed are those denoted *A1* and *A2* by Fergusson.¹¹ A Ge(Li) energy spectrum without coincidence with the NaI detectors is necessary to normalize the measurements.

In the angular distribution measurements (AD), the γ rays are detected by the Ge(Li) detector, which moved in the horizontal plane from 0° to 130° . The distance between target and the Ge(Li) detector is about 10 cm. The normalization between two runs was accomplished with a NaI detector.

III. EXCITATION CURVE ANALYSIS FOR THE 8.92 MeV LEVELS

The 55° yield curves of the $^{14}\text{N}(p, \gamma)^{15}\text{O}$ reaction are shown in Fig. 1 for the following γ rays from

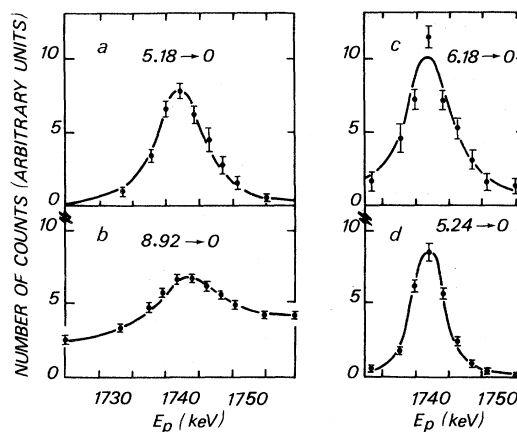


FIG. 1. Excitation functions at $\theta_{lab} = 55^\circ$ for the reaction $^{14}\text{N}(p, \gamma)^{15}\text{O}$ in the vicinity of the 1.742 MeV resonance. E_p is the incident proton energy.

the 1.742 MeV resonance: 5.18 MeV \rightarrow 0 (curve a), 8.92 MeV \rightarrow 0 (curve b), 6.18 MeV \rightarrow 0 (curve c) and 5.24 MeV \rightarrow 0 (curve d). The res \rightarrow 6.79 MeV \rightarrow 0 cascade was not studied because of the predominance of a nonresonant component.¹² The widths of the resonances, as deduced from these curves, are obviously different; this confirms the existence of a doublet. To determine the energies E_1, E_2 and the widths Γ_1, Γ_2 of its two components, it is necessary to decompose the experimental data into two resonance structures. The yield function Y employed in the fitting program is given by¹³

$$Y^j = \sum_{i=1,2} H_i^j \left[\tan^{-1} \left(\frac{E - (E_R)_i}{\frac{1}{2}\Gamma_i} \right) - \tan^{-1} \left(\frac{E - (E_R)_i - \xi}{\frac{1}{2}\Gamma_i} \right) \right], \quad (1)$$

with $H_i^j = k^j \{ [\sigma_i^j(E_R)_i \Gamma_i] / 2\epsilon \}$, if we assume that the differential cross sections $\sigma(E)$ follow the Breit-Wigner relation; E is the beam energy, $(E_R)_i$ and Γ_i are the energy and the width of the i th resonance, respectively, ϵ is the stopping cross section of the target material, and ξ is the energy loss of a proton in the target. The subscript i refers to the first ($i=1$) or the second ($i=2$) resonance, while j refers to the excitation curve fitted. Only relative measurements were performed, which explains the factor k^j . Equation (1) is valid only if interference between the resonances is neglected; the validity of this assumption is tested *a posteriori* with the parameters obtained from the best fits. Only a, c, and d curves are fitted; because of the presence of an important nonresonant background, which may interfere with the two resonances, the data (b) are not fitted, but the corresponding curve is plotted with the parameters obtained from the fit of the three other curves.

The quality of these fits is not very sensitive to the values of the main parameters Γ_1, Γ_2 , and ΔE (ΔE being the difference between the energies of the two resonances). Thus, it is interesting to use some of the values found in the previous elastic scattering study² where the width Γ_1 of the first resonance is determined with good precision because of the predominant contribution of this first resonance at backward angles. The value $\Gamma_1 = (3.5 \pm 0.3)$ keV is thus introduced in the fit of the γ -ray excitation data. For a given ΔE , the value of the width Γ_2 of the second resonance is adjusted so that the χ^2 value is minimized; this width is found to be 7.5 keV for $\Delta E = 0$ keV and then to increase with ΔE (to 11 keV for $\Delta E = 5$ keV). But, because of the small variation of the χ^2 values with ΔE , our excitation curves do not allow determination of ΔE and Γ_2 with good precision, as long as one of these two

parameters is not known with high accuracy. Thus, the elastic scattering curves of Ref. 2 were reanalyzed to obtain the possible variation interval for ΔE ; the suitable value is $\Delta E = (0.5 \pm 0.5)$ keV. If the γ -ray excitation data are fitted with values of Γ_1 and ΔE within their uncertainty limits, the best fit is obtained for $\Gamma_2 = 8$ keV (in agreement with the value of 8.5 keV deduced from the elastic scattering study). From the H_i^j values obtained in the fit, one can deduce the branching ratio for the cascades from the two levels, taking into consideration the branching ratio given by Evans *et al.*¹² who assumed the level to be single. However, the study of the χ^2 values versus H_1^j and H_2^j leads to very flat χ^2 surfaces. Therefore, the deduced values of H_i^j (corresponding to χ_{\min}^2) are obtained with errors ($> 50\%$) such that calculation of the branching ratio is not significant. We note that the study of the excitation functions is limited because of the very weak dependence of the different parameters upon the excitation curve shapes; however, one may conclude that the level at 8.92 MeV is a doublet and that the triple cascade 8.92 MeV \rightarrow 6.86 MeV \rightarrow 5.24 MeV \rightarrow 0 is fed only by the first member of the doublet, all other cascades being fed by both levels.

Krone and Fiarman,⁶ who decomposed their experimental (p, γ) data into two resonance structures, assuming the excitation function to have the same full width at half maximum (not given in their text), concluded that $\Delta E = 5$ keV. In order to illustrate the consequences of this assertion, we reexamined the previous elastic scattering results of Lambert *et al.*² with this ΔE value. Figure 2 shows the elastic scattering curves for two typical angles. Curve a is the result of Ref. 2; b and c are the results of the present reanalysis for $\Delta E = 5$ keV. Curve b is obtained assuming $\Gamma_1 = \Gamma_2 (= 3.5$ keV fixed by the excitation function at $\theta = 160^\circ$); the fit at $\theta = 70^\circ$ is very bad. Even if the width of the second resonance were greater (10 keV, curve c), the fit would be unsatisfactory. Therefore, the experimental data are inconsistent with the value $\Delta E = 5$ keV. This may be explained by the use of a solid target with high beam currents and build-up of carbon on the target, which would introduce errors into the branching ratio deduced in Ref. 6 from analysis of excitation curves.

IV. γ ANGULAR DISTRIBUTIONS AND CORRELATION RESULTS

8.92 MeV levels

This level fed by proton capture is a doublet and thus interferences between the members of this doublet occur. For this reason we have extended the calculation of Ferguson¹¹ to include the

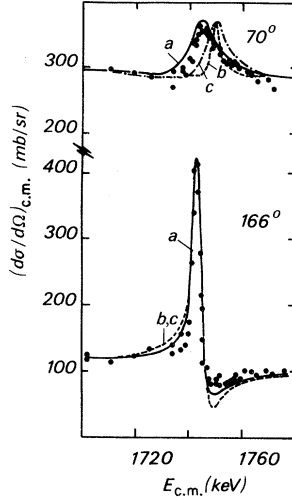


FIG. 2. Excitation functions for the $^{14}\text{N}(p,p)^{14}\text{N}$ reaction. The experimental points and the curve (a) which is the best fit obtained with $\Delta E=0.5$ keV, $\Gamma_{p_1}=3.5$ keV and $\Gamma_{p_2}=9.5$ keV are from Ref. 2. The other curves are obtained with $\Delta E=5$ keV, $\Gamma_{p_1}=3.5$ keV and $\Gamma_{p_2}=3.5$ keV (b) or 10 keV (c).

interference between two levels with different spins and parities. The schematic energy level diagram is shown in Fig. 3, which specifies the notations. For a i th cascade, the angular corre-

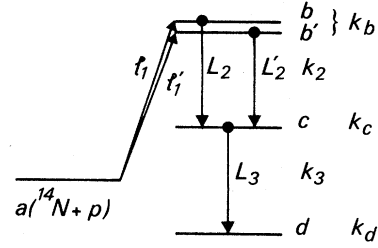


FIG. 3. Schematic energy level diagram for a $(p\gamma_2\gamma_3)$ reaction; a is one possible entrance channel spin; b, b' are the spins of the doublet fed by proton capture; c and d are the spins of the other levels; l and L are the orbital angular momenta of the incoming particle and of the outgoing γ ray, respectively; k_b, k_c , and k_d are the ranks of the density tensors for the final states (b, b'), c , and d , and k_2 and k_3 are the ranks of the efficiency tensors for the emitted radiations γ_2 and γ_3 .

lation is given by the summation of four terms $W_{bb'}$, where b (and b') takes the spin value of each member of the doublet

$$W(\theta_2, \theta_3, \varphi_{23}) \propto \sum_{bb'} W_{bb'}; \quad (2)$$

the angles θ_2, θ_3 , and φ_{23} are defined by Ferguson,¹¹ who gives the particular formula for $W_{bb'}$. The general expression is

$$W_{bb'} = \sum (-1)^{a+d+b-b'-k_b} \Theta_b \Theta_{b'} \bar{Z}(l_1 b l'_1 b', a k_b) \bar{Z}_1(\Lambda_3 c \Lambda'_3 c, d k_3) G_\gamma \begin{vmatrix} c & L_2 & b \\ c & L'_2 & b' \\ k_3 & k_2 & k_b \end{vmatrix} g_{a_1}^b g_{a_1'}^{b'} g_{L_2}^b g_{L_2'}^{b'} g_{L_3}^c g_{L_3'}^c \times \cos(\beta_b - \beta_{b'} + \xi_{l_1} - \xi_{l'_1}) \cos\beta_b \cos\beta_{b'} P_{k_b k_2 k_3}(\theta_2, \theta_3, \varphi_{23}) Q_{k_2} Q_{k_3}. \quad (3)$$

The summation extends over both values of a , over all possible values of $l_1, l'_1, L_2, L'_2, k_b, k_2$, and k_3 and over Λ_3, Λ'_3 which are the two possible values of L_3 . \bar{Z}, \bar{Z}_1 , and G_γ coefficients are tabulated in Ref. 11, Q_{k_2} and Q_{k_3} are the attenuation coefficients of the detectors, β_b is the resonance phase shift given by $\tan\beta_b = (E - E_R^b)/\frac{1}{2}\Gamma^b$, and ξ_{l_1} is the resonance phase shift associated with the incoming particle as defined by Blatt and Biedenharn.¹⁴ The proton width is defined as $\Gamma_p^b = \sum_{a_1} (\Gamma_{a_1}^b)_{a_1}$, $\Gamma_\gamma^b = \sum_L (\Gamma_\gamma^b)_L$ is the partial width for the (i)th outgoing γ ray, and Γ^b is the total width (approximated as Γ_p^b). Then

$$\Theta_b = \frac{(\Gamma_p^b \Gamma_\gamma^b)^{1/2}}{\Gamma^b}, \quad g_{a_1}^b = \frac{(\Gamma_p^b)_{a_1}^{1/2}}{(\Gamma^b)^{1/2}},$$

$$g_L^c = \frac{(\Gamma_\gamma^c)_L^{1/2}}{(\Gamma^c)^{1/2}} \quad [\epsilon = (bb'c)].$$

The absolute values of $g_{a_1}^b$ and $g_{a_1'}^{b'}$ are deduced

from the elastic scattering results² (these quantities are denoted g_{1s} in Ref. 2), their signs being unknown. The product $g_{a_1}^b \cdot g_{a_1'}^{b'}$ depends on the quantities $(g_{a_1}^b)^2$ and, in our case, on the products $\alpha g_{1/2,2}^b \cdot g_{1/2,1}^{b'}$ and $\beta g_{3/2,2}^b \cdot g_{3/2,1}^{b'}$ with $\alpha, \beta = \pm 1$. Thus, according to the values of α and β , four cases must be considered. Every case is included in our calculation. When the first radiation of the γ -ray cascade is not pure, the mixing ratios $g_{L_2+1}^b/g_{L_2}^b$ and $g_{L_2+1}^{b'}/g_{L_2}^{b'}$, are adjustable parameters. The values found for a minimum χ^2 are not given because of their great dependence of the choice of α and β and on the values of the γ width ratios Γ_γ^b/Γ^b . The value of the mixing ratio $g_{L_3+1}^c/g_{L_3}^c$ for the second γ ray in a cascade is generally well known.¹⁵⁻²¹

The results of the measurements are shown on the leftside of Figs. 4 and 5; error bars are essentially due to statistical errors and to the spectra analysis. They are important because of the

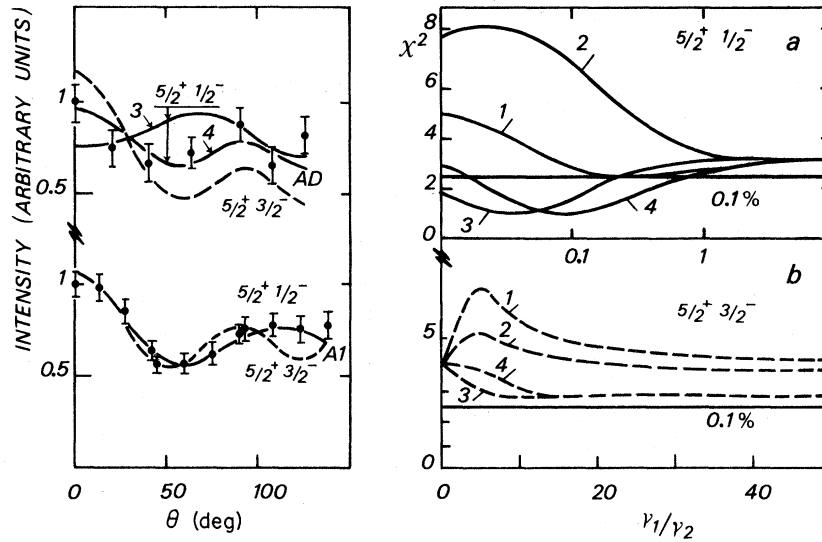


FIG. 4. Angular distribution data for the 8.92 MeV \rightarrow 5.18 MeV γ -ray and triple angular correlation (A1) for the 8.92 MeV \rightarrow 5.18 MeV \rightarrow 0 γ -ray cascade. The right part of the figure [(a) and (b)] shows the corresponding χ^2 curves versus the ratio of the γ widths of the two levels, with two sets of J^π determinations for the doublet. The values of the parameters α and β (see text) result in four cases: $(\alpha, \beta) = (1, 1)$ [1]; $(\alpha, \beta) = (-1, 1)$ [2]; $(\alpha, \beta) = (1, -1)$ [3]; $(\alpha, \beta) = (-1, -1)$ [4]. The left part of the figure shows the best fits for the two sets of spin determination. The dashed lines correspond to $J^\pi = (\frac{5}{2}^+, \frac{3}{2}^-)$ and solid lines to $J^\pi = (\frac{5}{2}^+, \frac{1}{2}^-)$. When the curves are not labeled they correspond to the [3][4] (undiscernible) cases.

low cross section in the capture channel. The experimental data are fitted by a χ^2 calculation; for each (i th) cascade from the 8.92 MeV level the χ^2 values are plotted, on the right parts of Figs.

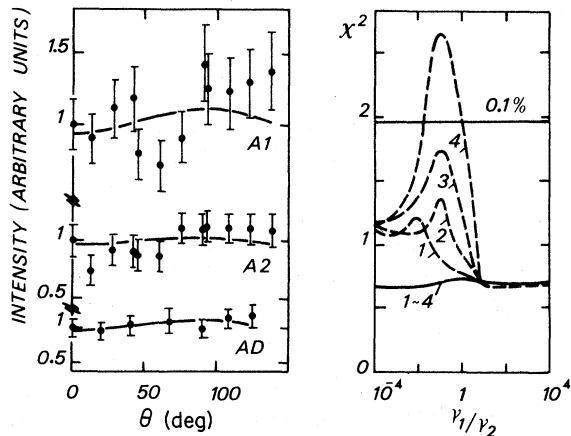


FIG. 5. Angular distribution data (AD) for the 6.18 MeV \rightarrow 0 radiation and triple angular correlation data (A1, A2) for the 8.92 MeV \rightarrow 6.18 MeV \rightarrow 0 γ -ray cascade. The right part of the figure shows the corresponding χ^2 curves versus the γ width ratio of the two levels. See Fig. 4 for the meaning of the solid and dashed lines and the labeling of the four possible (α, β) values. The left part of the figure shows the best fit for the two sets of spin determination (curves are indiscernible).

4 and 5, against the γ -width ratio $\gamma_1/\gamma_2 = \Gamma_{\gamma}^{5/2}/\Gamma_{\gamma}^{3/2}$ or $1/2$ for the four possible (α, β) values.

For the 8.92 MeV \rightarrow 5.18 MeV \rightarrow 0 cascade (Fig. 4), the asymmetry of the angular correlation A1 is clear and therefore the two γ rays are interfering. The first member of the doublet has $J^\pi = \frac{5}{2}^+$ and the two possible J^π for the second member are $\frac{1}{2}^-$ or $\frac{3}{2}^-$ (Ref. 2). Comparing the χ^2 curves, we can see that the $(\frac{5}{2}^+, \frac{3}{2}^-)$ determination is ruled out because the corresponding χ^2 curves [Fig. 4(b)] exceed the 0.1% χ^2 confidence limit, whereas the χ^2 curve $(\frac{5}{2}^+, \frac{1}{2}^-)$ [Fig. 4(a)] is below the 0.1% for $(\alpha, \beta) = (-1, -1)$ and $(\alpha, \beta) = (1, -1)$. The value of χ^2 is not very sensitive to the width ratio γ_1/γ_2 of the two levels; nevertheless, the value of this ratio is between 2×10^{-2} and 2×10^{-1} for the curves 3 and 4 on Fig. 4(a). We note that the value of γ widths calculated by Lie *et al.*⁸ are 1.7×10^{-3} eV for the $\frac{5}{2}^+_{(3)} \rightarrow \frac{1}{2}^+_{(1)}$ transition and 6.1×10^{-2} eV for the $\frac{1}{2}^-_{(2)} \rightarrow \frac{1}{2}^+_{(1)}$ transition, leading to a value of 2.8×10^{-2} for γ_1/γ_2 in good agreement with our results. The best fits are presented in the left part of the figure for the $(\frac{5}{2}^+, \frac{1}{2}^-)$ determination and for the ruled out $(\frac{5}{2}^+, \frac{3}{2}^-)$ determination.

For the 8.92 MeV \rightarrow 6.18 MeV \rightarrow 0 cascades (Fig. 5), the two determinations $(\frac{5}{2}^+, \frac{3}{2}^-)$ and $(\frac{5}{2}^+, \frac{1}{2}^-)$ for the spin and parity of the doublet are both consistent with experimental data. The $(\frac{5}{2}^+, \frac{3}{2}^-)$ determination having been ruled out above, no information on the γ -width ratio for the two levels

can be extracted from the χ^2 curves which are under the 0.1% χ^2 limit if we assume $J^\pi = \frac{5}{2}^+$ and $J^\pi = \frac{1}{2}^-$ for the members of the doublet.

For the study of the 8.92 MeV \rightarrow 6.86 MeV \rightarrow 5.24

MeV \rightarrow 0 cascade, we have performed the correlation between two γ rays (Fig. 6). The correlation function for a (*i*th) cascade is a summation of the type (2) with

$$W_{bb'}(\theta_n, \theta_4, \varphi_{n4}) \sim \sum (-1)^{b+b'+\lambda_n-a-e+k_b-k_c-1} \Theta_b \Theta_{b'} \bar{Z}(l_1 b l_1' b', a k_b) D \begin{pmatrix} c & L_2 & b \\ c & L_2' & b' \\ k_c & k_2 & k_b \end{pmatrix} \cdot D \begin{pmatrix} d & \Lambda_3 & c \\ d & \Lambda_3' & c \\ k_d & k_3 & k_c \end{pmatrix} \bar{Z}_1(\Lambda_4 d \Lambda_4' d, e k_d) \\ \times g_{a l_1}^b g_{a l_1'}^{b'} g_{L_2}^b g_{L_2'}^{b'} g_{\Lambda_3}^c g_{\Lambda_3'}^{c'} g_{\Lambda_4}^d g_{\Lambda_4'}^{d'} \cos \beta_b \cos \beta_{b'} \\ \times \cos[\beta_b - \beta_{b'} + \xi_{i_1} - \xi_{i_1'}] \mathcal{P}_{k_b k_n k_d}(\theta_n, \theta_4, \varphi_{n4}) Q_{k_n} Q_{k_d},$$

where *n* is the number of the detected radiation (*n* = 2 or 3; $\lambda_2 = L_2$, $\lambda_3 = \Lambda_3$). The summation has the same meaning as in Eq. (3), but in addition extends over k_4 and Λ_4 , Λ_4' which are the two possible value of L_4 . The coefficient

$$D \begin{pmatrix} \alpha & L_j & \beta \\ \alpha & L_j' & \beta' \\ k_\alpha & k_L & k_\beta \end{pmatrix}$$

is equal to

$$(-1)^{\beta'+\alpha-L_j'+1} \hat{\beta}' \hat{\beta} \hat{k}_\beta \hat{k}_L \hat{k}_\alpha \langle L_j L_j' 1 - 1 | k_L 0 \rangle \begin{cases} \alpha & L_j & \beta \\ \alpha & L_j' & \beta' \\ k_\alpha & k_L & k_\beta \end{cases} \quad \text{if } j=n$$

(using Clebsch-Gordan and 9*j* coefficients) or to

$$\hat{\beta}' \hat{\beta} \begin{cases} \beta & \alpha & L_j \\ \alpha & \beta' & k_\alpha \end{cases} \delta_{L_j L_j'} \delta_{k_\alpha k_\beta} \delta_{k_L 0} \quad \text{if } j \neq n$$

(using 6*j* coefficients). The quantity \mathcal{P} is defined from the associated Legendre polynomial P_k^K :

$$\mathcal{P}_{k_b k_n k_d}(\theta_n, \theta_4, \varphi_{n4}) = \frac{(-1)^{k_n}}{\hat{k}_4} \sum_{K \geq 0} (2 - \delta_{K0}) \langle k_b k_n 0 K | k_d K \rangle \left[\frac{(k_n - K)!(k_d - K)!}{(k_n + K)!(k_d + K)!} \right]^{1/2} P_{k_n}^K(\cos \theta_n) P_{k_d}^K(\cos \theta_4) \cos K \varphi_{n4}.$$

This formula is to be considered when the first or second γ ray is not detected. When the third γ ray is not detected, one must take the formula (3).

Figure 7 shows that the two determinations ($\frac{5}{2}^+$, $\frac{3}{2}^-$) and ($\frac{5}{2}^+$, $\frac{1}{2}^-$) are consistent with experimental data for this 8.92 MeV \rightarrow 6.86 MeV \rightarrow 5.24 MeV \rightarrow 0 cascade.

8.98 MeV level

This level is known to be ($\frac{3}{2}$, $\frac{1}{2}$)⁻ (Refs. 1, 3, and 4). Figure 8 shows the results for the 8.98 MeV \rightarrow 5.18 MeV \rightarrow 0 cascade. The angular distribution of the 8.98 MeV \rightarrow 5.18 MeV γ rays and the angular correlation in the A1 geometry are identical because of the spin $\frac{1}{2}$ of the 5.18 MeV level; their anisotropy forbids the $J^\pi = \frac{1}{2}^-$ determination for the 8.98 MeV level. Thus, the spin of this level

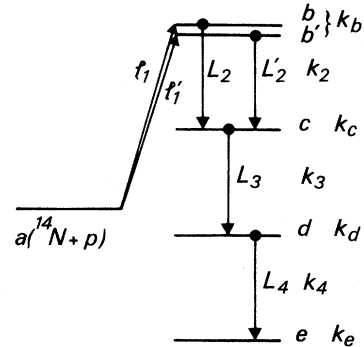


FIG. 6. Schematic energy level diagram for a ($p\gamma_2\gamma_3\gamma_4$) (γ_2 or γ_3 not seen) reaction. For the notations, see Fig. 3.

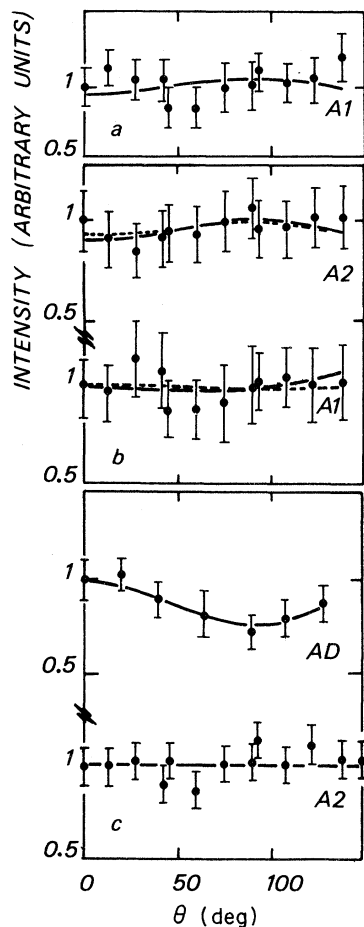


FIG. 7. Angular distribution (AD) data for the 8.92 MeV \rightarrow 6.86 MeV γ -ray and triple angular correlation (A1, A2) data for the 8.92 MeV \rightarrow 6.86 MeV \rightarrow 5.24 MeV \rightarrow 0 γ -ray cascade. The unobserved radiation is 8.92 MeV \rightarrow 6.86 MeV (a), 6.86 MeV \rightarrow 5.24 MeV (b), or 5.24 MeV \rightarrow 0 (c). See Fig. 4 for the meaning of the solid and dashed lines.

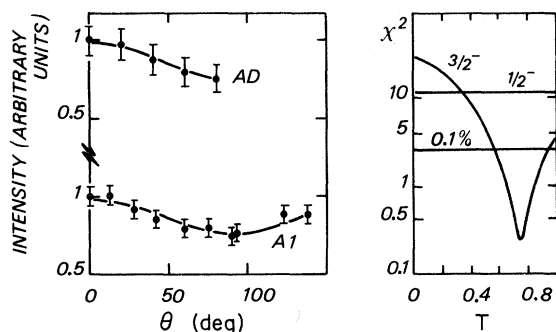


FIG. 8. Angular distribution (AD) data for the 8.98 MeV \rightarrow 5.18 MeV radiation and triple angular correlation (A1) data for the 8.98 MeV \rightarrow 5.18 MeV \rightarrow 0 γ -ray cascade. The right part of the figure shows the corresponding χ^2 curves versus the proportion T of reactions proceeding through spin channel $\frac{3}{2}$.

must be $\frac{3}{2}^-$. The χ^2 values are plotted against the proportion $T = g_{3/2,1}^2 / \sum a_l g_{al}^2$ of reactions proceeding through the channel spin $\frac{3}{2}$. The best fit is obtained for $T = 0.85^{+0.1}_{-0.3}$, in agreement with the value $T = 0.6$ given by Evans *et al.*¹² who studied the γ_0 angular distribution.

V. DISCUSSION

In this work no experimental value of the branching ratio is given because of the large uncertainties obtained in the analysis of the excitation curves. Nevertheless, it can be seen that all the cascades issued from the 8.92 MeV level, proceed from the two components of the doublet except for the 8.92 MeV \rightarrow 6.86 MeV \rightarrow 5.24 MeV \rightarrow 0 cascade which is fed only by the $\frac{5}{2}^+$ member. This conclusion agrees with the calculation of Ref. 8. No evidence of a 8.92 MeV \rightarrow 5.24 MeV \rightarrow 0 cascade is detected in our spectra; this is confirmed in Ref. 6 but is in contradiction with the theoretical prediction of Ref. 8 where this disagreement is explained by the presence of center of mass impurities.

8.92 MeV, $\frac{5}{2}^+$ state

This state was shown to be populated by the $^{13}\text{C}(^3\text{He}, n)^{15}\text{O}$ reaction^{3,4}; unfortunately the poor energy resolution did not yield the spin of the three members of the triplet (8.92–8.98 MeV). Etten and Lenz³ show that the presence of a state at 8.95 MeV with $J^\pi = \frac{5}{2}^+$ is not inconsistent with their data. The presence of a positive parity state populated by such a two-particle transfer reaction indicates a 1p-2h configuration. This assumption is consistent with the fact that this state is well excited in the one-particle transfer reaction $^{14}\text{N}(^{12}\text{C}, ^{11}\text{B})^{15}\text{O}$ (Ref. 22). Lie and Engeland⁸ suggested the existence of an experimental $\frac{5}{2}^+$ level at about 9 MeV in ^{15}O in correspondence with the $\frac{5}{2}$ member of the doublet at 9.15 MeV in ^{15}N . They identified this possible level with their third theoretical $\frac{5}{2}^+$ state at 7.75 MeV with a structure resulting from mixing of 1p-2h (35%) and 3p-4h (65%) configurations. Such a state is found by Saayman and de Kock,²³ but at an energy of 10.44 MeV, and with a pure 1p-2h configuration. Thus, the $\frac{5}{2}^+$ component of the 8.92 MeV doublet may be a candidate for the third theoretical $\frac{5}{2}^+$ level, although the differences between experimental and both theoretical energy positions are large (see the left part of Fig. 9). To test this correspondence, we have performed a Nilsson model²⁴ calculation of the positive parity states including the mixing of the rotational bands built up on the five orbits issued from the $1d_{5/2}$ and $1d_{3/2}$ shells; the deformation of the nucleus has been determined by minimizing the energy of each level. The $1s_{1/2}$

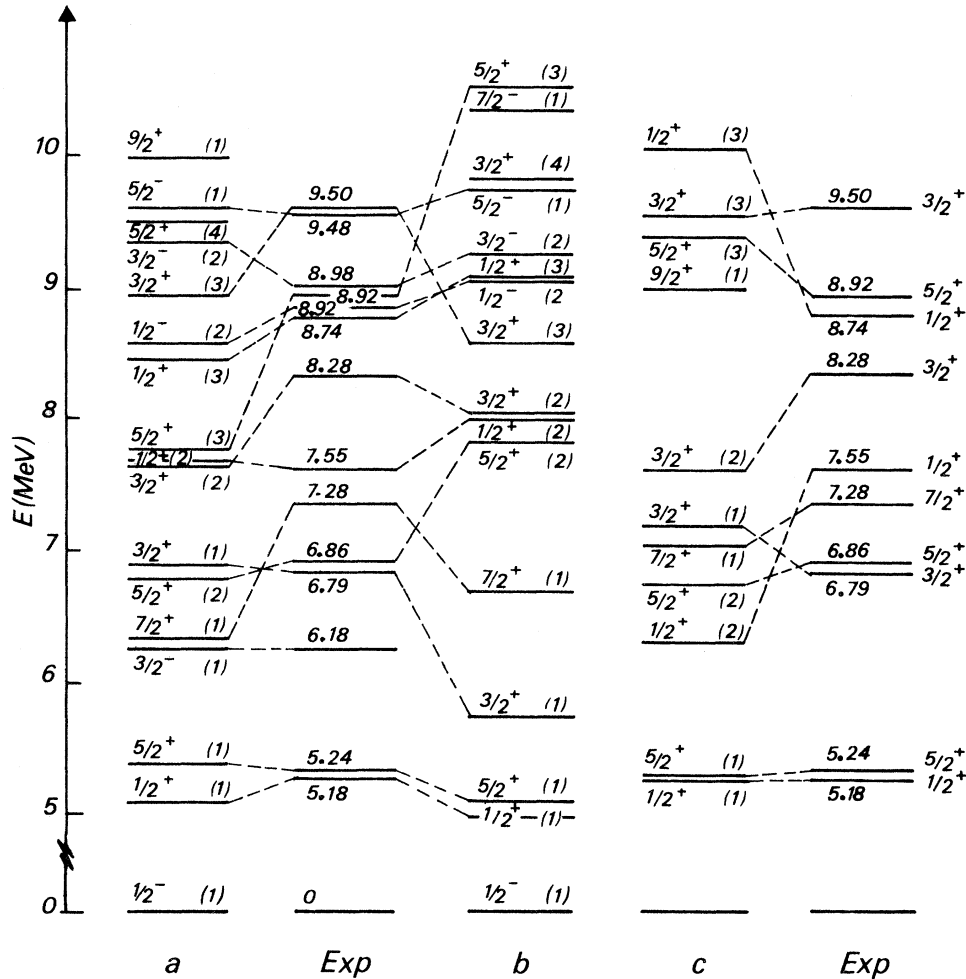


FIG. 9. Calculated and experimental levels for ^{15}O . The experimental data are taken from Ref. 1 and from this work. The theoretical results are from Ref. 8(a) or Ref. 23(b), column (c) shows the results of our calculation for positive parity states.

shell was found spherical and the energy of the associated level has therefore been calculated without any collective term. The right part of Fig. 9 shows that, up to 10 MeV, a fairly good agreement is obtained for the states found to have negative equilibrium deformations, which are well grouped about $\epsilon = -0.25$ (excepted for the third $\frac{3}{2}^+$ with $\epsilon = -0.15$). The only two levels ($\frac{1}{2}^+$) which are not well fitted by the model are found to have zero or slightly positive deformations. The correspondence between the experimental and theoretical energies of the $\frac{5}{2}^+$ states is quite satisfactory, which enforces the shell-model interpretation of the $\frac{5}{2}^+$ state at 8.92 MeV as the third $\frac{5}{2}^+$ theoretical level.

In ^{15}N , the $\frac{5}{2}^+$ level^{7,23} at 9.155 MeV is populated by the $^{14}\text{N}(d, p)^{15}\text{N}$ (Ref. 7), $^{14}\text{C}(d, n)^{15}\text{N}$ (Ref. 25), and $^{14}\text{N}(^{12}\text{C}, ^{11}\text{C})^{15}\text{N}$ (Ref. 22) reactions, which indicate a 1p-2h configuration, whereas the 3p-4h component appears in the $^{12}\text{C}(^7\text{Li}, \alpha)^{15}\text{N}$ reaction.²⁶

8.92 MeV, $\frac{1}{2}^-$ state

The presence of a $\frac{1}{2}^-$ state is not inconsistent with the results of the $^{13}\text{C}(^3\text{He}, n)^{15}\text{O}$ reaction studied by Hinderlitter and Lochstet.⁴ Thus, this state must have a 2p-3h configuration which is in agreement with the predictions of Refs. 8 and 23 for the second $\frac{1}{2}^-$ state in ^{15}O . The 2p-3h character of the $\frac{1}{2}^-$ (Refs. 7, 27, and 28) state at 9.224 MeV in ^{15}N is exhibited in the two-particle transfer $^{13}\text{C}(^3\text{He}, p)^{15}\text{N}$ reaction.²⁸

8.98 MeV, $\frac{3}{2}^-$ state

This state is populated through the $^{13}\text{C}(^3\text{He}, n)^{15}\text{O}$ reaction^{3,4} and is assigned $J^\pi = \frac{1}{2}^-$ by Etten and Lenz,³ whereas Hinderlitter and Lochstet⁴ assign $J^\pi = \frac{3}{2}^-$. The fact that this state is excited by this reaction indicates a 2p-3h configuration. The $\frac{3}{2}^-$ (Refs. 7, 27-29) state at 9.152 MeV in ^{15}N is well

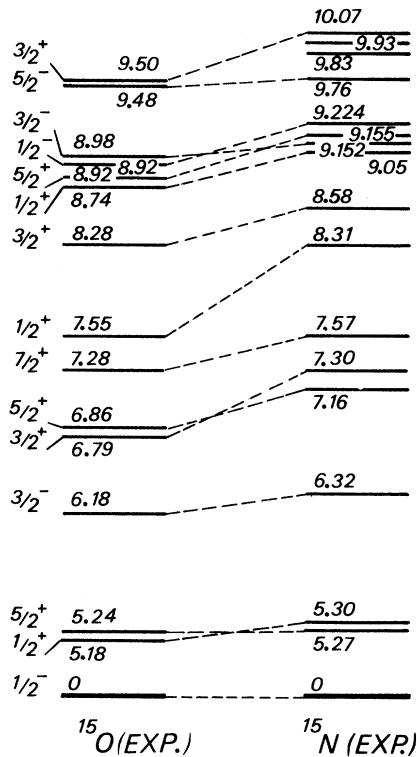


FIG. 10. The experimental energy spectra for ^{15}O (Refs. 1, 2, and this work) and ^{15}N (Ref. 7). The theoretical spectrum is from Ref. 8. Mirror levels are connected by dashed lines.

excited in the $^{13}\text{C}(^3\text{He}, p)^{15}\text{N}$ reaction which indicates a 2p-3h configuration, but a 4p-5h component is also exhibited in the study of the $^{11}\text{B}(^7\text{Li}, t)^{15}\text{N}$ reaction (Refs. 22, 30, and 31). It would be of interest to have results concerning four-particle transfer reactions populating the 8.98 MeV level in ^{15}O to illustrate the possible mixing of 2p-3h and 4p-5h configurations. This assumption is in contradiction to the conclusions of Refs. 8 and 23

where a predominance of 2p-3h configuration was found, the rest being 0p-1h configuration.

Isobaric analog states

The study of the $^{14}\text{N}(p, \gamma)^{15}\text{O}$ reaction following our previous conclusions from the $^{14}\text{N}(p, p)^{14}\text{N}$ reaction,² leads to the conclusion that the spin and parity of the two members of the doublet at 8.92 MeV in ^{15}O , are $J^\pi = \frac{5}{2}^+$ and $J^\pi = \frac{1}{2}^-$, while the 8.98 MeV level characteristics are $J^\pi = \frac{3}{2}^-$. Thus the $\frac{5}{2}^+$, 8.92 MeV, $\frac{1}{2}^-$, 8.92 MeV, and $\frac{3}{2}^-$, 8.98 MeV levels in ^{15}O are candidates to be the mirror states of the $\frac{5}{2}^+$, 9.155 MeV, $\frac{1}{2}^-$, 9.224 MeV, and $\frac{3}{2}^-$, 9.152 MeV levels, respectively, in ^{15}N .

This study does not permit the determination of the branching ratios for the two levels at 8.92 MeV in ^{15}O , and the branching ratios given by Krone and Fiarman⁶ are not applicable because of the larger value of ΔE employed; nevertheless, it is possible to affirm that all the cascades are fed by the two levels except the 8.92 MeV \rightarrow 8.86 MeV \rightarrow 5.24 MeV \rightarrow 0 cascade which is fed only by the $\frac{5}{2}^+$ level. Thus, the deexcitation scheme of the two 8.92 MeV levels is the same as that of the 9.155 and 9.224 MeV levels in ^{15}N (Ref. 1). The 8.98 MeV level in ^{15}O and the 9.152 MeV level in ^{15}N decays principally to the ground state. This and the comparison of the configuration of these three levels in ^{15}O and ^{15}N confirms that these states are mirror levels. Moreover, the neutron reduced widths γ_n^2 , deduced from the $^{14}\text{N}(d, p)^{15}\text{N}$ reaction⁷ and the proton reduced widths γ_p^2 deduced from the $^{14}\text{N}(p, p)^{14}\text{N}$ reaction^{1,2} are in good agreement for these analog states.

The correspondence between ^{15}O and ^{15}N levels up to 9.5 MeV in ^{15}O are summarized in Fig. 10.

The authors are indebted to Dr. C. Meynadier for his assistance in performing the experiments. They wish to thank Dr. P. Desgrolard for useful discussions.

¹F. Ajzenberg-Selove, Nucl. Phys. A152, 1 (1970).

²M. Lambert, O. Bersillon, B. Chambon, D. Drain, and J. L. Vidal, Nuovo Cimento Lett. 2, 1193 (1971).

³M. P. Etten and G. H. Lenz, Nucl. Phys. A179, 448 (1972).

⁴H. F. Hinderlitter and W. A. Lochstet, Nucl. Phys. A163, 661 (1971).

⁵J. L. Honsaker, W. J. McDonald, G. C. Neilson, and T. H. Hsu, in *Contributions to the International Conference on Properties of Nuclear States, Montreal, Canada, August 25-30, 1969* (Univ. of Montreal Press, Quebec, 1969), p. 299.

⁶R. W. Krone and S. Fiarman, Phys. Rev. C 6, 95 (1972).

⁷A. Amokrane, M. Allab, H. Beaumevielle, B. Faid,

O. Bersillon, B. Chambon, D. Drain, and J. L. Vidal, Phys. Rev. C 6, 1934 (1972).

⁸S. Lie, T. Engeland, and G. Dahll, Nucl. Phys. A156, 449 (1970); S. Lie and T. Engeland, *ibid.* A169, 617 (1971).

⁹H. M. Kuan, M. Hasinoff, W. J. O'Connell, and S. S. Hanna, Nucl. Phys. A151, 129 (1970).

¹⁰S. Bashkin and R. R. Carlson, Phys. Rev. 106, 261 (1957).

¹¹A. J. Ferguson, *Angular correlation Methods in Gamma-Ray Spectroscopy* (North-Holland, Amsterdam, 1965).

¹²A. E. Evans, B. Brown, and J. B. Marion, Phys. Rev. 149, 863 (1966).

- ¹³J. B. Marion, *Nuclear Data Tables* (National Academy of Science, Washington, D. C., 1960), Part 3.
- ¹⁴J. M. Blatt and L. C. Biedenharn, *Rev. Mod. Phys.* 24, 258 (1952).
- ¹⁵B. Povh and D. F. Hebbard, *Phys. Rev.* 115, 608 (1959).
- ¹⁶S. Gorodetzky, R. M. Freeman, A. Gallmann, and F. Haas, *Phys. Rev.* 149, 801 (1966).
- ¹⁷A. Gallmann, F. Haas, and N. Balaux, *Phys. Rev.* 151, 735 (1966).
- ¹⁸J. S. Lopes, O. Häusser, H. J. Rose, A. R. Poletti, and M. F. Thomas, *Nucl. Phys.* 76, 223 (1966).
- ¹⁹R. D. Gill, J. S. Lopes, B. C. Robertson, R. A. I. Bell, and H. J. Rose, *Nucl. Phys.* A106, 678 (1968).
- ²⁰R. Avida, M. B. Goldberg, Y. Horowitz, K. H. Speidel, and Y. Wolfson, *Nucl. Phys.* A172, 113 (1971).
- ²¹D. C. Kean and M. R. Wormald, *Can. J. Phys.* 52, 265 (1974).
- ²²N. Anyas-Weiss, J. C. Cornell, P. S. Fisher, P. N. Hudson, A. Menchaca-Rocha, D. J. Millener, A. D. Panagiotou, D. K. Scott, D. Strotman, D. M. Brink, B. Buck, P. J. Ellis, and T. Engeland, *Phys. Reports* 12C, 203 (1974).
- ²³R. Saayman and P. R. de Kock, *Z. Phys.* 266, 83 (1974).
- ²⁴S. G. Nilsson, *K. Dan. Vidensk. Selsk. Mat.-Fys. Medd.* 29, No. 16 (1955).
- ²⁵J. Bommer, M. Ekpo, H. Fuchs, K. Grabisch, and H. Kluge, *Nucl. Phys.* A251, 246 (1975).
- ²⁶I. Tserruya, B. Rosner, and K. Bethge, *Nucl. Phys.* A213, 22 (1973).
- ²⁷H. E. Stiefken, P. M. Cockburn, and R. W. Krone, *Nucl. Phys.* A128, 162 (1969).
- ²⁸C. E. Steerman and F. C. Young, *Nucl. Phys.* A192, 353 (1972).
- ²⁹J. C. Kim, H. S. Caplan, and I-O. Auer, *Phys. Lett.* 56B, 442 (1975).
- ³⁰K. Bethge, *J. Phys. (Paris)* 32, C6-87 (1971).
- ³¹El Bedewi, M. Shalaby, and S. Embaby, *J. Phys.* G 1, 534 (1975).